AGU PUBLICATIONS

Geophysical Research Letters

RESEARCH LETTER
10.1002/2015GL066015

Key Points:
- Evaluation of the winter frontal precipitation in CMIP5 models using objective front identification
- Frontal precipitation well represented on average but due to complex compensating factors
- Amplifying impact of fronts on rainfall intensity too high in models because of low biased total

Supporting Information:
- Tables S1 and S2

Correspondence to:
J. L. Catto,
jennifer.catto@monash.edu

Citation:
Catto, J. L., C. Jakob, and N. Nicholls (2015), Can the CMIP5 models represent winter frontal precipitation?, *Geophys. Res. Lett.*, *42*, 8596–8604, doi:10.1002/2015GL066015.

Received 31 AUG 2015
Accepted 30 SEP 2015
Accepted article online 5 OCT 2015
Published online 24 OCT 2015

Can the CMIP5 models represent winter frontal precipitation?

J. L. Catto[1], C. Jakob[2], and N. Nicholls[1]

[1]School of Earth, Atmosphere and Environment, Monash University, Clayton, Victoria, Australia, [2]Centre of Excellence for Climate Systems Science, School of Earth, Atmosphere and Environment, Monash University, Clayton, Victoria, Australia

Abstract Much of the day-to-day variability of rainfall in the midlatitudes is controlled by the passage of extratropical cyclones and their related fronts. A good representation of fronts and their associated rainfall in climate models is essential to have confidence in future projections of midlatitude precipitation. An objective front identification method has been applied to the data from ERA-Interim and 18 Coupled Model Intercomparison Project, version 5 (CMIP5) models and the fronts linked with daily precipitation estimates to investigate how winter front-related precipitation is represented in the models. While the front frequency is well represented, the frequency of frontal precipitation is too high and the intensity is too low, thus adding little bias to the rainfall total. Although the intensity of the modeled frontal precipitation is too low, the intensity of other precipitation is even lower; thus, the ratio of frontal precipitation to total precipitation is higher in the models than in the reanalysis.

1. Introduction

How the global distribution of precipitation and its variability will change in the future climate is a key topic of research highlighted by the World Climate Research Program. Changing characteristics of precipitation will have huge socioeconomic impacts, for example, on water availability, flood risk, and food production. Total global precipitation is expected to increase by approximately 2–3% per degree of warming [*Held and Soden*, 2006], due to a strong increase associated with global average surface temperature rise [*Trenberth et al.*, 2003] and a weaker suppression due to the atmospheric radiative heating [*Allen and Ingram*, 2002; *Dong et al.*, 2009; *Andrews et al.*, 2010]. However, the extremes are expected to intensify at a greater rate than the global average precipitation [*Allan and Soden*, 2008].

Much of the day-to-day variability of rainfall in the midlatitudes is controlled by the passage of extratropical cyclones and their related fronts. *Catto et al.* [2012] showed that over the midlatitudes up to 90% of annual precipitation is associated with fronts, with an average of around 70%, while *Hawcroft et al.* [2012] showed that a large proportion of North Atlantic storm track precipitation comes from extratropical cyclones. Fronts were also shown to be important for extreme precipitation events [*Catto and Pfahl*, 2013], especially when also related to warm conveyor belts [*Catto et al.*, 2015]. *Solman and Orlanski* [2014] investigated the relationship between changes in frontal activity and precipitation in the Southern Hemisphere (SH) midlatitudes over the past 40 years and found a strong correspondence between front frequency increases (decreases) and increased (decreased) precipitation. This relationship was also strong on an interannual basis. Since midlatitude total and extreme precipitation are strongly related to frontal activity, a good representation of fronts and their associated rainfall is a necessary condition for us to have confidence in model predictions of changes in midlatitude precipitation.

The frequency of occurrence of fronts was shown in *Catto et al.* [2014] to be fairly well represented by the models from the Coupled Model Intercomparison Project, version 5 (CMIP5), with some location biases consistent with storm track evaluation studies [*Zappa et al.*, 2013; *Chang et al.*, 2013]. *Catto et al.* [2013] applied the methodology of *Catto et al.* [2012] to data from the Australian Community Climate and Earth System Simulator (ACCESS) to evaluate the representation of fronts and their associated precipitation. They also performed an error decomposition similar to the methods of *Bony et al.* [2004] and *Williams and Tselioudis* [2007] and found that both frontal and nonfrontal precipitation occur too frequently and with overall too low intensity. A number of studies have found similar issues when considering any type of precipitation [*Dai*, 2006; *Sun et al.*, 2006; *Stephens et al.*, 2010].

The main aim of the present study is to evaluate the precipitation associated with fronts in a number of state-of-the-art climate models from the CMIP5 archive with the goal to answer the following questions.

1. What is the contribution to the model precipitation biases from front-related precipitation?
2. How are front-related precipitation biases related to the frequency and intensity of frontal precipitation?
3. Is the ratio between frontal and total precipitation (the amplifying effect) well represented in the models?
4. How do the models represent the proportion of precipitation from fronts?

The focus is on the winter seasons in each hemisphere (i.e., December, January, and February (DJF) in the Northern Hemisphere (NH) and June, July, and August (JJA) in the SH).

2. Methods and Data

The automated front identification method of *Berry et al.* [2011] following the techniques of *Hewson* [1998] used in this study has recently been used in a number of other studies [e.g., *Catto et al.*, 2014]. The brief description here closely follows the details in those papers.

The front identification has been applied to 6-hourly data from the European Centre for Medium Range Weather Forecasting reanalysis data set, ERA-Interim [*Dee et al.*, 2011] for DJF 1997/1998–2007/2008 and JJA 1997–2008, and to model data from the CMIP5 archive [*Taylor et al.*, 2012] (a list of the models used is given in the supporting information and is based on the availability of the required data) for DJF 1980/1981–2004/2005 and JJA 1980–2005. Frontal points are identified using a thermal front parameter described by *Renard and Clarke* [1965], based on 850hPa wet bulb potential temperature. A threshold value of $-8 \times 10^{-12}\mathrm{Km}^{-2}$ is used to mask the field, and frontal points are identified where the gradient of the thermal front parameter equals 0. These points are linked into contiguous fronts and output on a 2.5° grid.

The fronts are linked with daily precipitation estimates automatically using the method of *Catto et al.* [2012]. For the ERA-Interim fronts, daily precipitation estimates are taken from the Global Precipitation Climatology Project (GPCP) 1° daily data set [*Huffman et al.*, 2001]. The satellite- and gauge-based data from GPCP have been chosen since ERA-Interim precipitation is a forecast variable and tends to underestimate daily and monthly precipitation accumulations [e.g., *Szczypta et al.*, 2011; *de Leeuw et al.*, 2015], although the time series correlate well with GPCP [*Szczypta et al.*, 2011]. The precipitation data are interpolated onto the same grid as the fronts. If a grid box contains greater than 1mm of 24h accumulated precipitation, a search is performed in that and the neighboring eight grid boxes. If a front occurs at any of the four 6-hourly analysis times during the 24h accumulation period, the precipitation is allocated as being associated with fronts. The results found using the fronts from ERA-Interim and precipitation from GPCP are our best estimate of the observations and will be used as a base against which the models are evaluated.

As stated above, there is a well-known issue with climate models in that they tend to produce very small amounts of precipitation very frequently [e.g., *Sun et al.*, 2006; *Stephens et al.*, 2010]. During winter, in the models examined here, precipitation occurs on 100% of days or close to it (see Table S2 in the supporting information), whereas in GPCP it occurs 61% and 52% of days in the SH and NH, respectively. In order to better align the frequency of modeled rainfall with observations, we examined the use of a precipitation threshold of 1mm/day, which brings the model estimates of the proportion of precipitating days closer to the satellite estimates (see Table S2 in the supporting information). To test the rationality of using such a threshold, the percentage of total seasonal precipitation coming from days with intensities less than 1mm/day has been calculated for GPCP and for the multimodel mean for the winter midlatitudes. For SH JJA, only 2.3% of total GPCP precipitation comes from days with precipitation less than 1mm/day, with a value of 5.0% for the multimodel mean. For NH DJF the values are 6.9% and 12.2% for GPCP and the models, respectively. While there are some differences between GPCP and the models, overall the precipitation less than 1mm/day contributes a small amount to the total seasonal precipitation. For these reasons, the threshold of 1mm/day is used throughout the rest of the study.

In this study, the method of *Catto et al.* [2013] has been used to decompose the total precipitation error in the model. This method is similar to the decomposition techniques of *Williams and Tselioudis* [2007] and *Zappa et al.* [2014]. In this case there are two regimes of interest: the frontal precipitation regime and the nonfrontal precipitation regime. The total precipitation error in the model can be broken down into the components

related to the frequency of occurrence of the regime (frontal or nonfrontal) and to the intensity of precipitation associated with that regime. The total error E_p can be represented as

$$E_p = P_m - P_o \tag{1}$$

$$E_p = F_{f,m}I_{f,m} + F_{nf,m}I_{nf,m} - F_{f,o}I_{f,o} - F_{nf,o}I_{nf,o} \tag{2}$$

$$E_p = \Delta F_f I_{f,o} + F_{f,o}\Delta I_f + \Delta F_f \Delta I_f + \Delta F_{nf} I_{nf,o} + F_{nf,o}\Delta I_{nf} + \Delta F_{nf}\Delta I_{nf} \tag{3}$$

where the subscript f represents the frontal regime, nf represents the nonfrontal regime, m represents the model, and o the observations. F is the frequency of occurrence of the precipitation regimes, and I is the intensity of precipitation associated with each regime. The terms ΔF and ΔI represent the difference between the model and the observations for the frequency and intensity, respectively. Since our focus is on the impact of frontal precipitation biases, only the first three terms are described in the next section.

3. Precipitation Error and Contribution From Frontal Precipitation

Figure 1a shows the multimodel mean winter precipitation bias relative to GPCP. In the NH, the bias is fairly small in absolute terms, with positive biases of up to 1.5mm/day over the east of the North Atlantic and negative biases of a similar magnitude over the Labrador Sea. In percentage terms, these are biases of about 30% (Figure 1b). The precipitation is up to 2.5mm/day (50%) too high over the Kuroshio current (Figures 1a and 1b) and over much of the western half of the U.S.

In the SH, over most of the midlatitudes, there are positive biases of up to 2mm/day, corresponding to up to 50% higher precipitation than in GPCP. To the east of South America the precipitation is too low in the models (Figures 1a and 1b).

The location of the large precipitation biases in the multimodel mean (i.e., over the storm track regions) suggests that these errors could be associated with fronts. In order to explore this, the sum of the first three terms in equation (3), i.e., the frontal precipitation error terms, is shown in Figure 1c. Over most regions the frontal precipitation errors are small; there are negative contributions to the error over the North Atlantic region, at high latitudes in the SH, and to the east of South America, and there are positive contributions to the error over the midlatitude Indian Ocean, to the east of New Zealand, and over the Kuroshio Current. Even though the frontal contribution to the errors are mostly smaller than the total, this does not necessarily mean that the frontal precipitation is well represented for the correct reason.

The decomposition of the precipitation bias splits the frontal precipitation contribution into that from the frequency (Figure 2a) and the intensity (Figure 2b), as well as the cross terms (Figure 2c). Considering first the NH, the positive bias over the Kuroshio current region (Figure 1) has a large positive contribution from the frequency of frontal precipitation (Figure 2a). Figure 3a shows that in this region, the frequency of frontal influence is too high by about 6% of days, and to the south of this the frequency is too low by up to 14%. Over this whole region, however, the frequency of frontal precipitation is much too high compared to ERA-Interim/GPCP (Figure 3b). Therefore, the positive contribution to the total precipitation bias from the frequency of frontal precipitation is slightly related to too many fronts but more strongly related to there being too many fronts producing precipitation. Over the North Atlantic region, there is a positive contribution from the frequency of frontal precipitation (Figure 2a), again associated with too many fronts producing precipitation (Figure 3b), particularly in the high-latitude eastern end of the storm track. In the NH the contributions to the total precipitation error from the intensity of frontal precipitation are negative almost everywhere, compensating for the frequency errors.

In the SH, the decomposition shows that there is a positive contribution to the overall positive bias from the frequency in frontal precipitation. This is up to about 2mm/day to the east of South Africa. In this region the frequency of fronts themselves (Figure 3a) is well represented (even slightly low), but the frequency of frontal precipitation is too high (Figure 3b). There is a similar pattern over most of the SH midlatitudes; however, the larger positive contribution to the precipitation bias to the northeast of New Zealand is related to too many fronts as well as too many rainy fronts (Figures 3a and 3b).

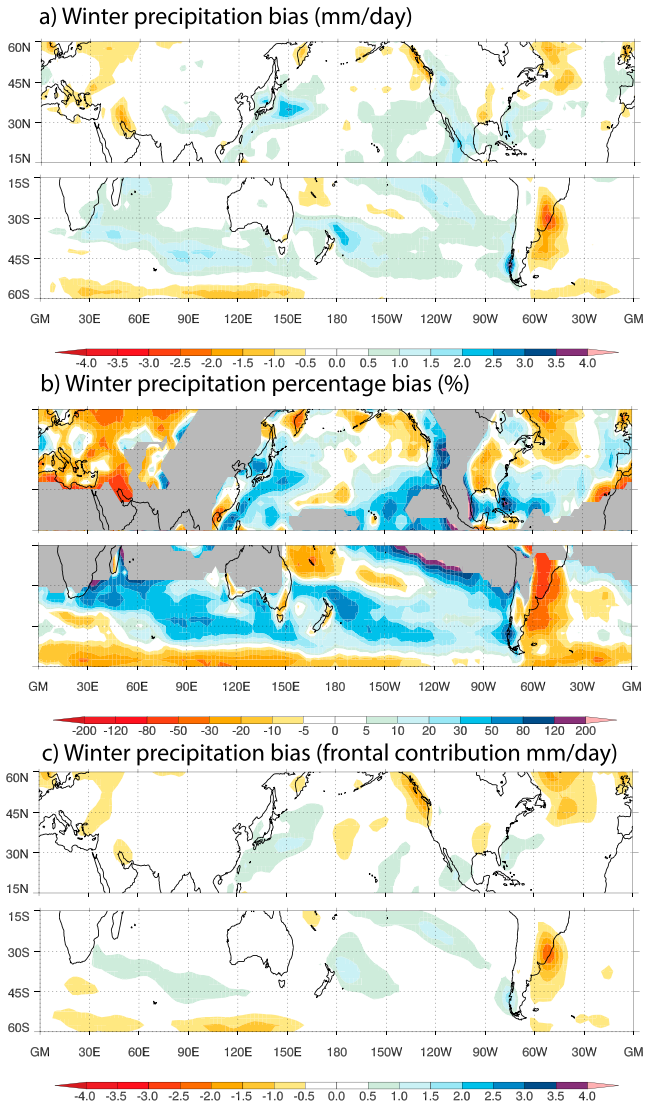

Figure 1. Multimodel mean winter precipitation bias (NH DJF and SH JJA). (a) Absolute bias (mm/day), (b) percentage bias (%), and (c) frontal contribution to absolute bias (mm/day). In Figure 1b regions where the climatological winter precipitation is less than 1mm/day are masked in grey.

In the SH midlatitudes there is everywhere a negative contribution to the precipitation error from the intensity of frontal precipitation. This partly offsets the positive contribution from the frequency. The negative contributions from intensity of frontal precipitation are mainly seen to be associated with the higher latitude errors and those to the east of South America. This is because in other regions where the frontal precipitation intensity is higher (for example, over North West Australia, not shown), the frequency of the fronts is small enough that this does not play a large role in the overall precipitation errors.

In the multimodel mean precipitation error decomposition, there is compensation between positive contributions from the frequency and negative contributions from the intensity. It is important to consider whether these figures are dominated by one model or if all the considered models show the same patterns. Figure 2d shows the winter midlatitude area-averaged values of the error decomposition for each model. In both hemispheres, it can be seen that the area-averaged total precipitation biases are small in all the models—in the NH they are typically less than ±0.2mm/day and in the SH less than ±0.4mm/day. Term 1, which represents the contributions from the frequency of frontal precipitation, is positive in all models in both hemispheres. Term 2, which represents the contribution from the intensity of frontal precipitation, is negative on average in all of the models. In almost all models the contributions are larger in the SH. Term 3 is the cross term and

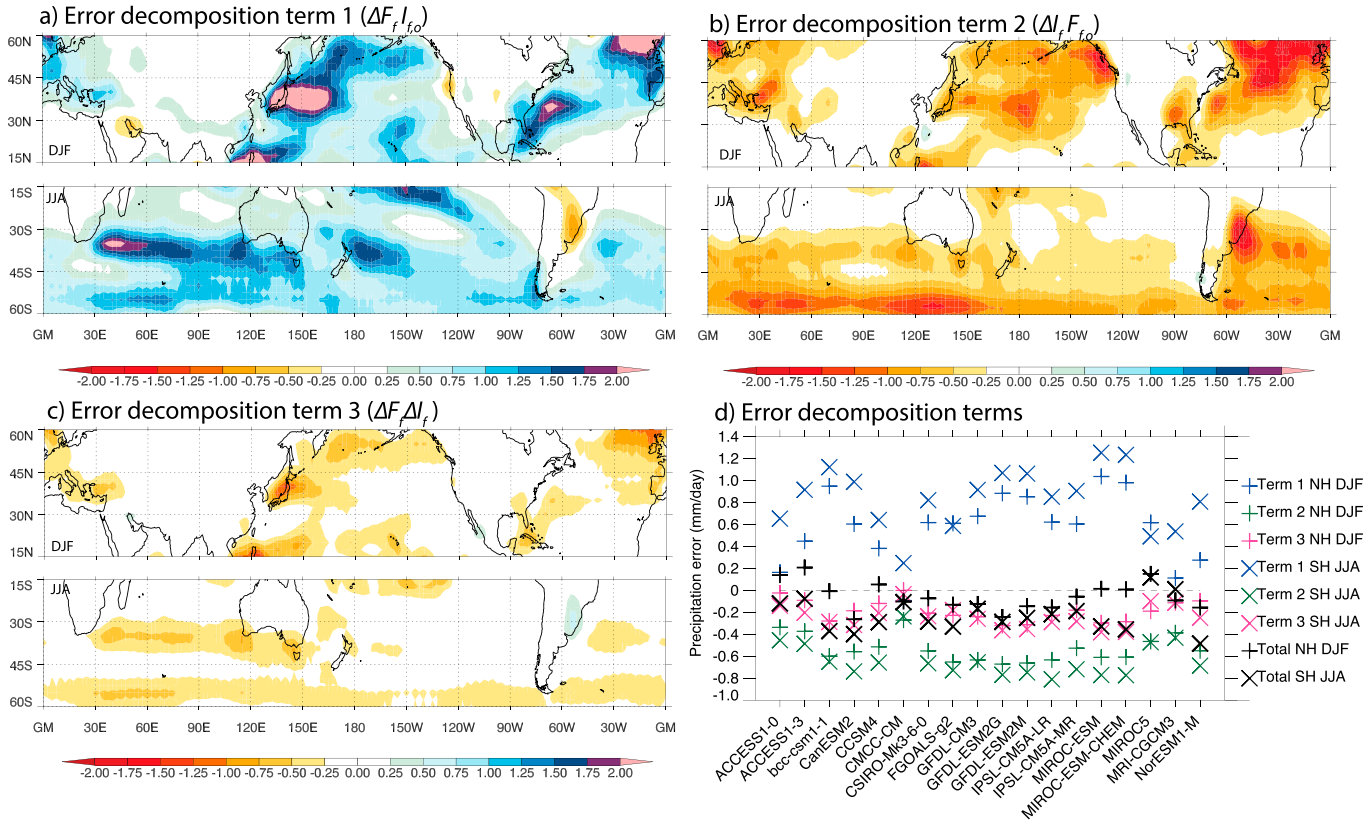

Figure 2. Winter error decomposition terms related to frontal precipitation considering precipitation greater than 1mm/day. (a) $\Delta F_f I_{f,o}$, (b) $F_{f,o} \Delta I_f$, and (c) $\Delta F_f \Delta I_f$. (d) NH and SH midlatitude (30–60°) mean error decomposition terms for each of the models considered.

is negative almost everywhere. The negative contributions due to intensity are not compensated for by positive frequency errors in the SH as well as in the NH. While there is some variability between the magnitude of the decomposition terms from the different models, overall they show the same picture as that seen in the ACCESS atmosphere only simulation from *Catto et al.* [2013]. The model with the smallest frontal precipitation errors is CMCC-CM. This model has the highest atmospheric resolution of those included (0.75°) and therefore may be better at representing the frontal circulation features and precipitation processes.

4. Dynamical Impact of Fronts on Precipitation

The intensity of frontal precipitation has previously been shown to be higher than nonfrontal precipitation using GPCP [*Catto et al.*, 2012], and most extreme precipitation events in the midlatitudes are associated with fronts [*Catto and Pfahl*, 2013]. This indicates that fronts have the effect of amplifying the intensity of precipitation over some background state, but it is important to understand if the models can represent this amplifying effect. In order to answer this question, we have calculated a frontal amplification factor (A_f), which is the ratio of frontal precipitation intensity to total precipitation intensity (I_f/I_{all}). The spatial pattern from ERA-Interim/GPCP (colors) and the multimodel mean error (contours) are shown in Figure 3c. In the observational estimate, A_f shows quite a uniform distribution over the midlatitudes with values between 1 and 1.1. The area-averaged value for the NH winter is 1.075 and for the SH winter is 1.083. This means that over the midlatitudes on average the frontal precipitation is about 8% higher than the total precipitation. There are regions with higher values, such as over the Kuroshio Current and the Gulf Stream and in the subtropical ocean regions of the SH and over Australia. In the multimodel mean over much of the midlatitudes, the values of A_f are fairly well represented. Over the more subtropical regions and over regions of warm sea surface temperatures, for example, in the South Pacific Convergence Zone and over the Gulf Stream and Kuroshio current, the values are too high by up to 0.5. In almost all the models the area-averaged values of A_f over the midlatitudes (30–60°) are too high. This indicates that when a front is present, it is having too much of an effect

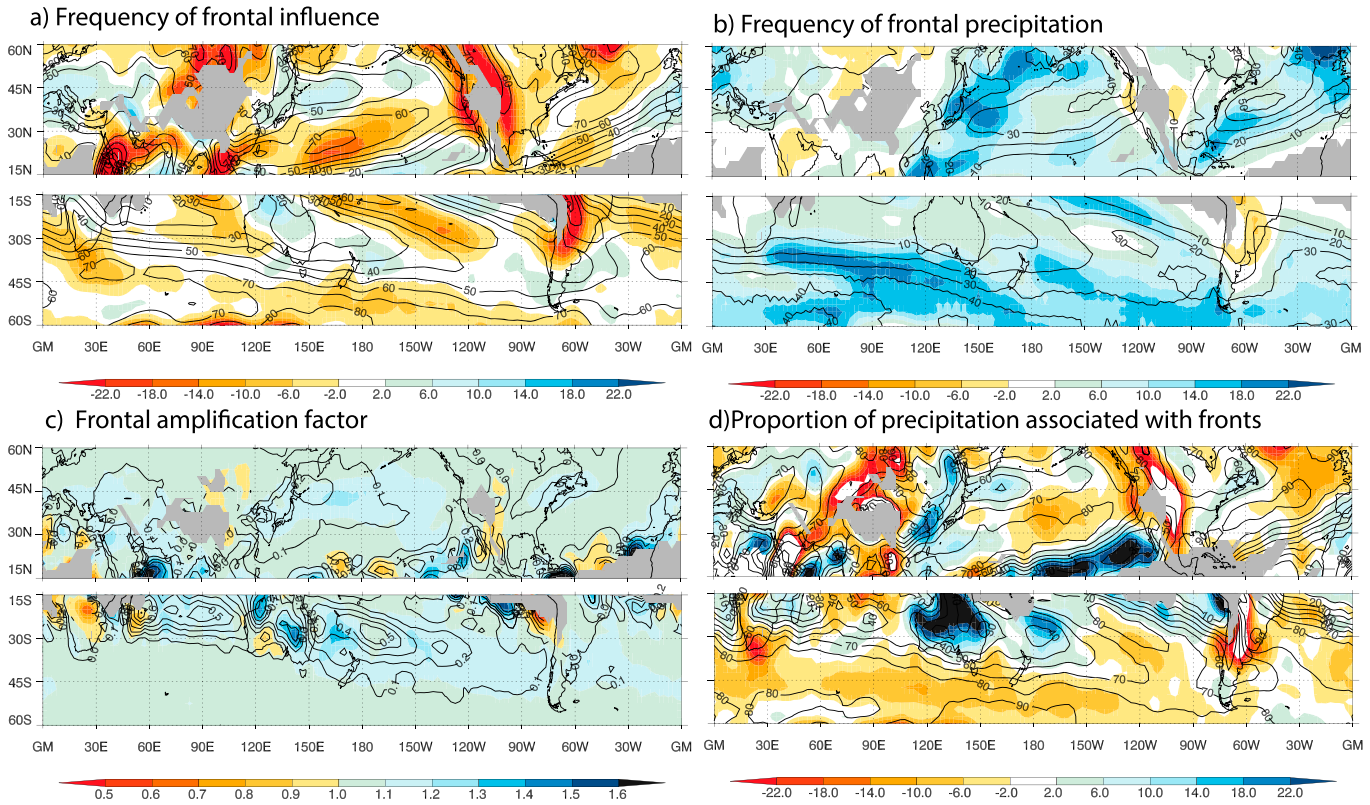

Figure 3. Winter (DJF in NH and JJA in SH) (a) frequency of frontal influence (proportion of days that a grid box is influenced by a front; %) for ERA-Interim (contours) and multimodel mean bias (colors), (b) frequency of frontal precipitation (proportion of days that have frontal precipitation in a grid box; %) for ERA-Interim (contours) and multimodel mean bias (colors), (c) frontal amplification factor (A_f=I_f/I_{all}; nondimensional) for ERA-Interim (colors) and multimodel mean bias (contours) , and (d) proportion of precipitation associated with fronts (%) for ERA-Interim (contours) and multimodel mean bias (colors).

on the precipitation. It is important to understand how this overamplification is consistent with the intensity of the frontal precipitation being too low.

The error in A_f is actually associated with a too low estimate of the frontal precipitation intensity and an even lower estimate of the overall precipitation intensity. This is demonstrated for all the models in Figure 4 by the percentage intensity error for frontal precipitation (black and blue crosses) and for total precipitation (black and blue circles). Almost every model has a larger error in the total than the frontal precipitation. This leads to a value of A_f that is too high compared to ERA-Interim/GPCP. This also shows that the frontal precipitation is better represented in the models than the nonfrontal precipitation.

This amplification effect has been explored further by considering precipitation at higher thresholds than 1mm/day. The intensities of frontal and total precipitation have been calculated for various thresholds up to 20mm/day and the A_f calculated. In the observations, as the threshold increases, the value of A_f asymptotes to 1. This is because in the midlatitudes it is very hard to get heavy precipitation without the influence of a front; therefore, the value of I_f comes very close to I_{all}. The models also show the same effect, indicating that much of the heaviest precipitation in the models comes from fronts. At higher precipitation thresholds the models are also better at representing the mean frontal and total precipitation intensity (Figure 4).

5. Proportion of Precipitation From Fronts

A valuable measure of the influence of fronts on precipitation is the proportion of total precipitation associated with fronts [*Catto et al.*, 2012]. Given the strongly compensating errors in the frequency and intensity of frontal precipitation, and the enhanced dynamical amplification of the frontal precipitation, it is interesting to investigate how this measure is represented in the models.

Figure 3d shows the proportion of precipitation above 1mm/day associated with fronts from ERA-Interim/GPCP and the multimodel mean bias for winter in each hemisphere. The pattern of the proportion of

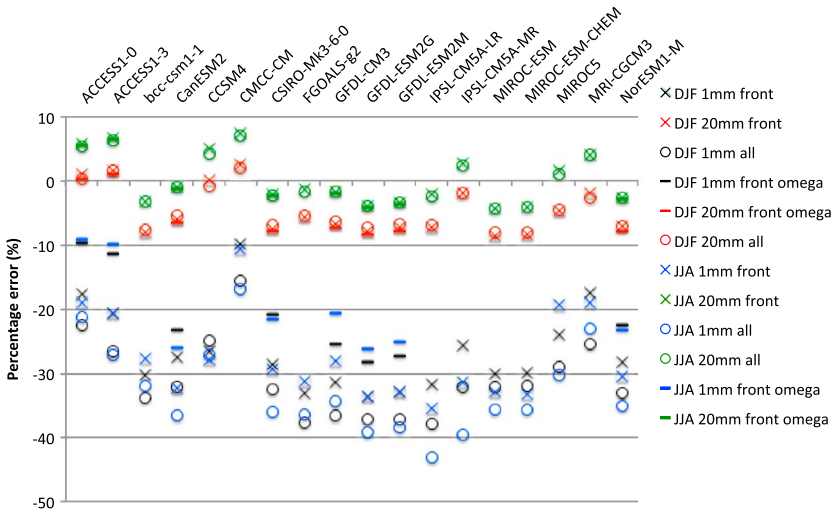

Figure 4. The percentage error in precipitation intensity averaged over the winter midlatitudes (30–60°) for each model. Errors are shown for frontal and total precipitation with a threshold of 1mm/day and a threshold of 20mm/day and also for frontal precipitation with both thresholds but considering the extra criterion of upward motion (omega).

precipitation associated with fronts is quite well represented in the multimodel mean. However, in much of the SH midlatitudes, this is underestimated by about 10% . This appears to be at least partly associated with a slightly lower frequency of frontal influence (seen in Figure 3a). The proportion of precipitation associated with fronts over most of Australia is much too large, related to the high frequency of front-related precipitation seen (Figure 3b) and the very low climatological precipitation values in this region (not shown). In the NH midlatitudes there are some large errors in the proportion of precipitation from fronts. Over the eastern end of the North Atlantic storm track, there is a negative bias of up to about 10%. Even though the frequency of wet fronts is high here (Figure 3b), the frequency of frontal influence is too low, as is the intensity of the frontal precipitation. There is also a region on the southern edge of the Pacific storm track where there is a large positive error of over 20%. This is a region of low climatological precipitation of less than 2mm/day in the multimodel mean (not shown) and is a region where there are too many fronts (Figure 3a).

6. Concluding Discussion

By employing an automated front identification scheme, we have investigated the representation of winter frontal precipitation in 18 of the CMIP5 historical simulations and the contribution of any errors to the total precipitation errors. Although the frontal contribution to the total error is quite small, the analysis shows that this is related to compensating errors. The frequency of frontal precipitation is too high in all the models, but the intensity is too low. In the models, when a front is present, the intensity of the precipitation is amplified over the background value by more than that in the observations. However, the frontal precipitation intensity is still too low but is being amplified over the background value that is biased even lower. Despite the compensating errors and the overamplification of the frontal precipitation over the background value, the proportion of precipitation associated with fronts is too low over much of the midlatitudes.

A surprising result from the study was the small observed A_f. We investigated the impact of our method of allocating precipitation to fronts by including an extra criterion of ascent in the precipitation grid box. This acts to eliminate precipitation found in grid boxes experiencing subsidence. The area-averaged A_f over the midlatitudes from ERA-Interim/GPCP when the ascent criterion is included is 1.16 for NH and 1.20 for SH, indicating that the frontal precipitation intensity is increased when including the ascent criterion. This is likely a result of excluding precipitation from shallow convection behind a front, which in the 2.5° data set would be light. We were only able to test the effect of the ascent criterion on a small number of the models due to data availability. Including this criterion reduces the percentage errors in precipitation intensity from the models when considering the low threshold of 1mm/day (Figure 4). This indicates that some of the intensity bias is associated with there being very light rainfall occurring in subsidence in the models that is not present in the observations. Since I_{all} is the same in the calculation of A_f, the model errors in A_f when including the ascent criterion are even larger.

The results of this study are consistent with previous climate model evaluations of the characteristics of precipitation [e.g., *Sun et al.*, 2006; *Wilcox and Donner*, 2007; *Stephens et al.*, 2010]. By considering the contribution to the total precipitation biases in the models from the frontal precipitation, we have shown that although the frontal precipitation biases are small, this is due to compensating errors. Given that we find the frontal precipitation intensity to be better represented in the models than is the total precipitation, we could place more confidence in future projections of frontal precipitation, including the extremes, which, in the midlatitudes are influenced more by large-scale processes than convection [*O'Gorman and Schneider*, 2009].

Frontal precipitation is often associated with large-scale uplift along the tilted isentropes [e.g., *Browning*, 1986]. *Catto et al.* [2010] found that the isentropes within extratropical cyclones in a climate model were not steep enough, while *Govekar et al.* [2014] found the ascent in SH model cyclones too weak, and *Zappa et al.* [2013] show that North Atlantic storms are dynamically too weak, aspects that could all lead to frontal precipitation that is weaker than observed. A future study will investigate the link between the characteristics of the fronts and the precipitation associated with them and how these features are represented in climate models. An important aspect for future work is not just to consider grid point analysis but also to aim to understand individual systems and whether the life cycle of cyclones and their associated fronts and precipitation is well represented in the models.

Acknowledgments

This study was supported by the Australian Research Council through the Linkage Project grants LP0883961 and LP130100373, the Discovery Project grant DP0877417, the ARC Centre of Excellence for Climate System Science (grant CE110001028), and the Discovery Early Career Researcher Award (grant DE140101305). The front identification algorithm was kindly provided by Gareth Berry. We acknowledge the World Climate Research Programme's Working Group on Coupled Modelling, which is responsible for CMIP, and we thank the climate modeling groups (listed in supporting information Table S1 of this paper) for producing and making available their model output. For CMIP the U.S. Department of Energy's Program for Climate Model Diagnosis and Intercomparison provides coordinating support and led development of software infrastructure in partnership with the Global Organization for Earth System Science Portals. CMIP5 data are available at http://pcmdi9.llnl.gov/esgf-web-fe/, and ERA-Interim data are available at http://apps.ecmwf.int/datasets/. J.L.C. would also like to thank Harvey Ye for all his help in downloading the CMIP5 data.

References

Allan, R. P., and B. J. Soden (2008), Atmospheric warming and the amplification of precipitation extremes, *Science*, *321*, 1481–1484, doi:10.1126/science.1160787.

Allen, M. R., and W. J. Ingram (2002), Constraints on future changes in climate and the hydrological cycle, *Nature*, *419*, 224–232.

Andrews, T., P. M. Forster, O. Boucher, N. Bellouin, and A. Jones (2010), Precipitation, radiative forcing and global temperature change, *Geophys. Res. Lett.*, *37*, L14701, doi:10.1029/2010GL043991.

Berry, G., M. J. Reeder, and C. Jakob (2011), A global climatology of atmospheric fronts, *Geophys. Res. Lett.*, *38*, L04809, doi:10.1029/2010GL046451.

Bony, S., J. L. Dufresne, H. Le Treut, J. J. Morcrette, and C. A. Senior (2004), On dynamic and thermodynamic components of cloud changes, *Clim. Dyn.*, *22*, 71–86.

Browning, K. A. (1986), Conceptual models of precipitation systems, *Weather Forecasting*, *1*, 23–41.

Catto, J. L., and S. Pfahl (2013), The importance of fronts for extreme precipitation, *J. Geophys. Res.*, *118*, 1–11, doi:10.1002/jgrd.50852.

Catto, J. L., L. C. Shaffrey, and K. I. Hodges (2010), Can climate models capture the structure of extratropical cyclones?, *J. Clim.*, *23*, 1621–1635.

Catto, J. L., C. Jakob, G. Berry, and N. Nicholls (2012), Relating global precipitation to atmospheric fronts, *Geophys. Res. Lett.*, *39*, L10805, doi:10.1029/2012GL051736.

Catto, J. L., C. Jakob, and N. Nicholls (2013), A global evaluation of fronts and precipitation in the ACCESS model, *Aust. Meteorol. Ocean. Soc. J.*, *63*, 191–203.

Catto, J. L., N. Nicholls, C. Jakob, and K. L. Shelton (2014), Atmospheric fronts in current and future climates, *Geophys. Res. Lett.*, *41*, 7642–7650, doi:10.1002/2014GL061943.

Catto, J. L., E. Madonna, H. Joos, I. Rudeva, and I. Simmonds (2015), Global relationship between fronts and warm conveyor belts and the impact on extreme precipitation, *J. Clim.*, doi:10.1175/JCLI-D-15-0171.1.

Chang, E. K. M., Y. J. Gua, X. M. Xia, and M. H. Zheng (2013), Storm-track activity in IPCC AR4/CMIP3 model simulations, *J. Clim.*, *26*, 246–260, doi:10.1175/JCLI-D-11-00707.1.

Dai, A. (2006), Precipitation characteristics in eighteen coupled climate models, *J. Clim.*, *19*, 4605–4630.

de Leeuw, J., J. Methven, and M. Blackburn (2015), Evaluation of ERA-Interim reanalysis precipitation products using England and Wales observations, *Q. J. R. Meteorol. Soc.*, *141*, 798–806, doi:10.1002/QJ.2395.

Dee, D. P., et al. (2011), The ERA-Interim reanalysis: Configuration and performance of the data assimilation system, *Q. J. R. Meteorol. Soc.*, *137*, 553–597.

Dong, B., J. M. Gregory, and R. T. Sutton (2009), Understanding land-sea warming contrast in response to increasing greenhouse gases. Part I: Transient adjustment, *J. Clim.*, *22*, 3079–3097.

Govekar, P., C. Jakob, and J. L. Catto (2014), The relationship between clouds and dynamics in Southern Hemisphere extratropical cyclones in the real world and a climate model, *J. Geophys. Res.*, *119*, 6609–6628, doi:10.1002/2013JD020699.

Hawcroft, M. K., L. C. Shaffrey, K. I. Hodges, and H. F. Dacre (2012), How much Northern Hemisphere precipitation is associated with extratropical cyclones?, *Geophys. Res. Lett.*, *39*, L24809, doi:10.1029/2012GL053866.

Held, I. M., and B. J. Soden (2006), Robust responses of the hydrological cycle to global warming, *J. Clim.*, *19*, 5686–5699.

Hewson, T. D. (1998), Objective fronts, *Meteorol. Appl.*, *5*, 37–65.

Huffman, G. J., R. F. Adler, M. Morrissey, D. T. Bolvin, S. Curtis, R. Joyce, B. McGavock, and J. Susskind (2001), Global precipitation at one-degree daily resolution from multi-satellite observations, *J. Hydrometeor.*, *2*, 36–50.

O'Gorman, P., and T. Schneider (2009), The physical basis for increases in precipitation extremes in simulations of 21st-century climate change, *Proc. Natl. Acad. Sci. U.S.A.*, *106*, 14,773–14,777.

Renard, R. J., and L. C. Clarke (1965), Experiments in numerical objective frontal analysis, *Mon. Weather Rev.*, *93*, 547–556.

Solman, S. A., and I. Orlanski (2014), Poleward shift and change of frontal activity in the Southern Hemisphere over the last 40 years, *J. Atmos. Sci.*, *71*, 539–552.

Stephens, G. L., T. L'Ecuyer, R. Forbes, A. Gettlemen, J.-C. Golaz, A. Bodas-Salcedo, K. Suzuki, P. Gabriel, and J. Haynes (2010), Dreary state of precipitation in global models, *J. Geophys. Res.*, *115*, D24211, doi:10.1029/2010JD014532.

Sun, Y., S. Solomon, A. Dai, and R. W. Portmann (2006), How often does it rain?, *J. Clim.*, *19*, 916–934.

Szczypta, C., J. C. Calvet, C. Albergel, G. Balsamo, S. Boussetta, D. Career, S. Lafont, and C. Meurey (2011), Verification of the new ECMWF ERA-Interim reanalysis over France, *Hydrol. Earth Syst. Sci.*, *15*, 647–666, doi:10.5194/hess-15-647-2011.

Taylor, K. E., R. J. Stouffer, and G. A. Meehl (2012), An overview of CMIP5 and the experiment design, *Bull. Am. Meteorol. Soc.*, *93*, 485–498, doi:10.1175/BAMS-D-11-00094.1.

Trenberth, K. E., A. Dai, R. M. Rasmussen, and D. B. Parsons (2003), The changing character of precipitation, *Bull. Am. Meteorol. Soc.*, *84*, 1205–1217.

Wilcox, E. M., and L. J. Donner (2007), The frequency of extreme rain events in satellite rain-rate estimates and an atmospheric general circulation model, *J. Clim.*, *20*, 53–69.

Williams, K. D., and G. Tselioudis (2007), GCM intercomparison of global cloud regimes: Present-day evaluation and climate change response, *Clim. Dyn.*, *29*, 231–250.

Zappa, G., L. C. Shaffrey, and K. I. Hodges (2013), The ability of CMIP5 models to simulate North Atlantic extratropical cyclones, *J. Clim.*, *26*, 5379–5396, doi:10.1175/JCLI-D-12-00501.1.

Zappa, G., M. K. Hawcroft, L. C. Shaffrey, E. Black, and D. J. Brayshaw (2014), Extratropical cyclones and the projected decline of winter Mediterranean precipitation in the CMIP5 models, *Clim. Dyn.*, doi:10.1007/s00382-014-2426-8.